Available online at www.sciencedirect.com
ScienceDirect
journal homepage: www.elsevier.com/locate/he

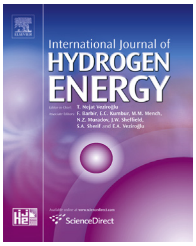

# A novel candidate for hydrogen storage: Ca-decorated zigzag $C_3N$ nanotube

*Farzad Molani* [a,*], *Seifollah Jalili* [b,c], *Jeremy Schofield* [d]

[a] *Department of Chemistry, Sanandaj Branch, Islamic Azad University, P. O. Box 6616935391, Sanandaj, Iran*
[b] *Department of Chemistry, K. N. Toosi University of Technology, P. O. Box 1541849611, Tehran, Iran*
[c] *Computational Physical Sciences Research Laboratory, School of Nano-Science, Institute for Research in Fundamental Sciences (IPM), P.O. Box 19395-5531, Tehran, Iran*
[d] *Chemical Physics Theory Group, Department of Chemistry, University of Toronto, 80 Saint George Street, Toronto, Ontario, Canada M5S 3H6*

## ARTICLE INFO

*Article history:*
Received 11 January 2016
Received in revised form
6 March 2016
Accepted 19 March 2016
Available online 8 April 2016

*Keywords:*
Hydrogen storage
Adsorption
Calcium decorated $C_3N$ nanotube
First principle calculations

## ABSTRACT

In order to search high-capacity hydrogen storage media, first-principles calculations were performed. Ca-decorated on perfect and defective $C_3N$ nanotube as a new adsorbent for $H_2$ molecules were studied. It was found that the Ca-decorated on defective nanotube can adsorb up to eight $H_2$ molecules with the average binding energy of 0.11 eV/$H_2$. Interaction of Ca atom with the nanotubes and $H_2$ molecules are explained by Dewar coordination and Kubas interaction, respectively. Furthermore, the binding energy of the Ca atom on the defective nanotubes at least two times larger than the perfect one. Hence, clustering of the Ca atom on the nanotubes can be prevented by defect region.

## Introduction

Nowadays discovery of novel materials for sustainable, renewable, and clean energy as like as hydrogen is an interested research. Carbon-based nanomaterials have been widely studied for their application in hydrogen storage [1,2]. Since pristine carbon nanostructures are chemically too inert to be useful for practical hydrogen storage (HS) [3–5], it is necessary to active these nanostructures by coating, doping, and/or introducing defects [5–27]. Clustering of metal atoms is a major drawback in utilizing metal-coated nanostructures as HS materials which reduces the gravimetric and volumetric density [5,10,20].

Among metals considered, the Ca atom exhibits the most favorable hydrogen adsorption characteristics in terms of the binding energy ($E_{bind}$) and uptake capacity [10,11,17,28–34]. Because of a moderate cohesive energy ($E_{coh}$) for the Ca atom (i.e. −1.84 eV/atom) [35], compare with other alkali earth metals (AEMs) and transition metals (TMs), the clustering of the Ca atoms can be effectively hindered by this proper energy. The $E_{bind}$ of the Ca atom on carbon nanotube (CNT), graphene, and $C_{60}$, are almost 0.88 [10], 1.1 [33,36], and 1.3 eV/Ca [17], respectively. All these $E_{bind}$ are less than the $E_{coh}$ of the bulk Ca. Scientists showed that the clustering of the Ca atoms could be suppressed by doping or introducing defects [29,33,37]. Ao and Peeters showed that N-doped and applying

---

* *Corresponding author*. Tel.: +98 914 442 3308; fax: +98 87 33247713.
E-mail addresses: f.molani@iausdj.ac.ir (F. Molani), sjalili@kntu.ac.ir (S. Jalili), jmschofi@chem.utoronto.ca (J. Schofield).

http://dx.doi.org/10.1016/j.ijhydene.2016.03.118

an electric field have catalytic effects on the hydrogenation of carbon nanostructures, which can be a promising HS media with reversible hydrogen adsorption/desorption [14,15,38]. By means of DFT calculations, Rao et al. have studied Ca-doped N-substituted defective graphene and its potential application in $H_2$ storage [27]. They determined that the N-edged defects in graphene can enhance the binding energy of metals [27]. Furthermore, Mananghaya showed that the N-doped CNT enhanced chemical functionalization of all TMs suggesting a considerable reduction of clustering of metal atoms over the metal decorated nanotube. Strong binding of hydrogen molecule to the TMs on N-doped CNT was observed [25]. In addition to above modifications, finding new backbone materials to increase the $E_{bind}$ beyond the $E_{coh}$ is an alternative approach to avoid the clustering effect.

Multi-walled carbo-nitride nanotubes were synthesized by pyrolyzing ferrocene/melamine mixture [39]. Hales et al. have recently investigated structural and thermodynamic stability of small $C_xN$ nanotubes with $x = 1$, 2, 3, 5, and 7 [40]. Furthermore, many studies on $C_3N$ nanotube ($C_3$NNT) have newly been done [41–43]. Our previous study showed that defects have impact role on the structural and electronic properties of $C_3$NNT [41]. Unconstrained structure optimization of $C_3$NNT with an atom vacancy leads to the formation of a new bond, perpendicular to the tube axis and the system is reconstructed to a five-membered and a nine-membered ring with a dangling bond or under-coordinated atom (UA) just around the local defect region [41]. We also showed that the carbon vacancy ($C_\upsilon$) defect is more stable than the nitrogen vacancy ($N_\upsilon$) defect [41] and respect to CNT, graphene, $C_{60}$, and $B_{80}$ [42], $C_3$NNT is a better adsorbent for alkali metals (AMs).

In continue to the previous studies, the study of the interaction of Ca atom with $C_3$NNT was setting as a goal. To achieve our goal, we implemented a systematic search for high-capacity HS media consisting of Ca-decorated on the perfect or defective $C_3$NNT. To understand how this new backbone and vacancy defect effects on the Ca adsorption, the structural and electronic properties of the each structures were investigated.

## Computational details

First-principle calculations based on spin polarized density functional theory (DFT) were performed using the PWSCF code [44]. The exchange-correlation was described with the Perdew Burke Ernzerhof within the generalized-gradient approximation (GGA–PBE) [45]. The Monkhorst Pack meshes [46] of 1 × 1 × 9 were used in sampling the Brillouin zone of a tetragonal supercell of 20 Å × 20 Å × 17.08 Å containing 96 carbon atoms and 32 nitrogen atoms, with the length of $c$ equal to twice the periodicity of the (8,0) nanotube. Energy cutoff for the plane waves was set to 600 eV. All the structures were fully relaxed until atomic forces were less than 0.01 eV/Å. Furthermore, the $E_{bind}$ for the Ca atom to the nanotubes and the $E_{ads}$ of $H_2$ molecules on the adsorbents are given by $E_{bind} = E_{Ca@tube} - (E_{Ca} + E_{tube})$ and $E_{ads} = (E_{(nH2 + Ca@tube)} - (E_{(nH2)} + E_{(Ca\text{-}tube)}))/n$, respectively, where $E_{Ca}$, $E_{tube}$, $E_{(nH2)}$, $E_{Ca@tube}$, and $E_{(nH2 + Ca@tube)}$ are the total energy of Ca atom, Ca on the nanotube, isolated $H_2$ molecule, the nanotube, and adsorbed system, respectively. n is the number of adsorbed $H_2$ molecules. In order to charge analysis, Löwdin method was used [47]. It is notice that a negative (positive) value for charge transfer (CT) indicates that atom loses (gain) charge density. Furthermore, the work function ($\Phi$) is the minimum energy required to extract one electron from the surface to a point in the vacuum [35]. Field emission in semiconductors strongly depends on the $\Phi$ value [35].

## Results and discussion

### Ca-decorated $C_3$NNT

The optimized structures of Ca atom on perfect and defective tubes are shown in Fig. 1. In the perfect case, the Ca atom would rather to adsorb on center of hexagon ring consisting of four C atoms and two N atoms (4C–2N), regardless of initial positions. Interestingly, center of hexagon ring in graphene, CNT, $C_{60}$, and $BC_7$ is also the most favorable site to adsorption of the Ca atom [10,29,33,36]. Furthermore, center of the 4C–2N ring in the $C_3$NNT is also appropriate site for the AMs [42]. The structural and electronic parameters for the Ca-decorated $C_3$NNT are listed in Table 1. In the perfect form, minimum distance ($d_{min}$) between the Ca atom and C and N atoms are 2.79 and 2.41 Å, respectively. Bond lengths of C1–C2 and C2–N are elongated to 1.42 and 1.48 Å. These elongations are justified by the net CT about 0.33 |e| from the Ca atom to the nanotube. In both defective structures, Ca atom would rather to adsorb on nano-membered ring, as depicted in Fig. 1. From Table 1, new bond between Ca atom and nearest atom in $C_\upsilon$ and $N_\upsilon$ structures are about 2.22 and 2.26 Å, respectively. Since the nanotube gets some charges, bond lengths around the defect region are increased. The Ca atom on the $C_\upsilon$ and $N_\upsilon$ nanotubes lose 0.50 and 0.46 |e|, respectively.

Now, to discuss the chemical nature of the interaction of Ca atom with the nanotubes, the partial density of states (PDOS) of the complexes and calculated CT of the Ca atom are illustrated in Fig. 1 and Table 1, respectively. The results revealed that the energy gaps of the *Ca@perfect*, *Ca@Cυ*, and *Ca@Nυ* are 0.25, 0.64, and 0.06 eV, respectively. From CT and the existence of an unoccupied peak of the Ca atom above the Fermi level (see Fig. 1(I)–(III)), it can be deduced that the Ca atom in the system is in a cationic state and can act as a charge acceptor from other molecules such as hydrogen molecules. The induced positive charge of the Ca atom increases in the order of *perfect* < *Nυ* < *Cυ*, which correlated with their reactivity and the order of their $E_{bind}$, as interpreted from Table 1. The maximum CT and absolute value of $E_{bind}$ were also obtained for the *Ca@Cυ*. As seen in Table 1, the Ca *s* orbital on the *perfect*, *Cυ*, and *Nυ* structures loses 0.60, 0.92, and 0.89 |e|, respectively. In other hand, the Ca *d* orbital gets 0.26, 0.40, and 0.41 |e| from the *perfect*, *Cυ*, and *Nυ* structures, respectively. Interestingly, the Ca *p* orbital doesn't impact participate in the bonding mechanism. As interpreted from Fig. 1(I)–(III) and Table 1, the bonding originates by mixing of Ca 4*s* and 3*d* orbitals with the nanotubes 2*p* orbital, and simultaneously, there exists a donation and back donation between the metal and the nanotubes. Upon this findings, the bonding between the Ca atom and the nanotube obey Dewar

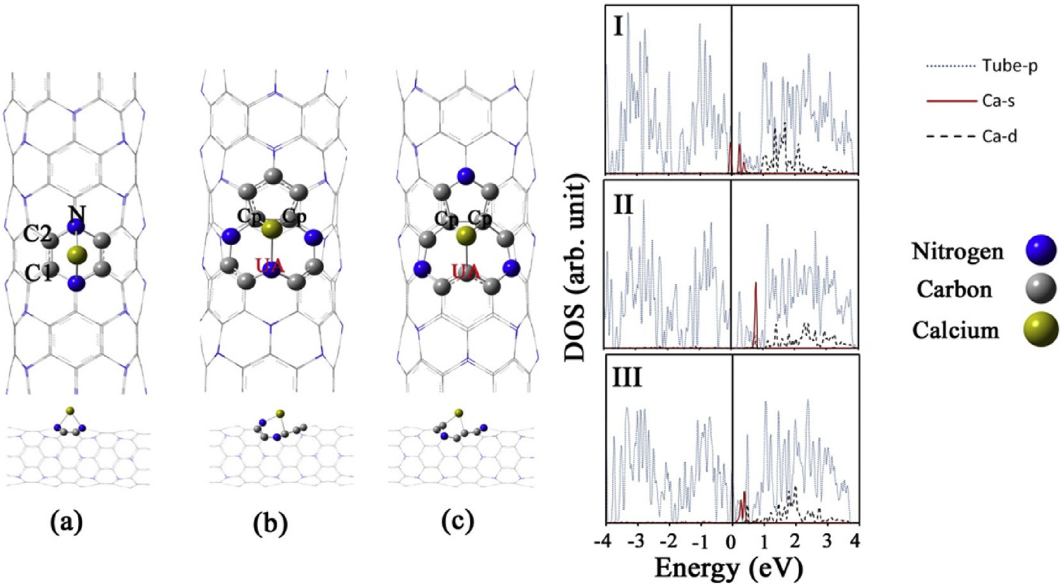

**Fig. 1 – Left panel: The optimized structures of the Ca atom on (a) perfect, (b) $C_v$, and (c) $N_v$ nanotubes. Right panel: Partial density of states (PDOS) for (I) Ca@perfect, (II) Ca@Cv, (III) Ca@Nv. Fermi level is set to zero.**

**Table 1 – Calculated minimum distance of Ca atom with the nanotube ($d_{min}$(Ca-tube)) and carbon atom in pentagon ring ($d_{min}$(Ca–$C_P$)), bond length of UA to nearest carbon atom (L(UA-C)), bond length between carbon atoms in pentagon ring (L(Cp–Cp)), energy gap ($E_{gap}$), binding energy ($E_{bind}$), charge transfer of s, p, and d orbitals of the Ca atom ($CT_{(s)}$), ($CT_{(p)}$), and ($CT_{(d)}$), respectively, and work function (Φ) for the Ca atom on $C_3$NNT. A negative value for CT indicates that the Ca atom lose charge density. Values in parenthesis are related to before Ca adsorption.**

| System | $d_{min}$(Ca-tube) (Å) | $d_{min}$(Ca-Cp) (Å) | L(UA-C) (Å) | L(Cp–Cp) (Å) | $E_{gap}$ (eV) | $E_{bind}$ (eV) | $CT_{(s)}$ \|e\| | $CT_{(p)}$ \|e\| | $CT_{(d)}$ \|e\| | Φ (eV) |
|---|---|---|---|---|---|---|---|---|---|---|
| Ca@perfect | 2.41 | – | – | – | 0.25 (0.32) | −1.17 | −0.60 | +0.01 | +0.26 | −1.82 (−2.28) |
| Ca@$C_v$ | 2.22 | 2.45 | 1.43 (1.38) | 1.46 (1.40) | 0.64 (0.10) | −3.8 | −0.92 | +0.02 | +0.40 | −1.78 (−2.15) |
| Ca@$N_v$ | 2.26 | 2.44 | 1.41 (1.35) | 1.55 (1.51) | 0.06 (0.26) | −2.47 | −0.89 | +0.02 | +0.41 | −1.61 (−2.20) |

coordination [48]. Moreover, the $E_{bind}$ of the Ca atom on the *perfect*, *Cv*, and *Nv* structures are −1.17, −3.80, and −2.47 eV/Ca, respectively and exothermic. The $E_{bind}$ of the Ca atom on the *perfect* tube is stronger than CNT [10,11], N-doped [11], graphene [33,36], MgO (100) [49], while is weaker than $BC_7$ [29], carbyne [30], $B_{80}$ [32], $C_{60}$ [50], and graphyne [51]. The $E_{bind}$ of Ca to the perfect form is less than the $E_{coh}$ of the bulk Ca. As a result, the Ca-cluster will form in practice which will affect on the gravimetric density of $H_2$. To solve this problem, we should introduce defects on the $C_3$NNT to increase the $E_{bind}$ of the Ca beyond the $E_{coh}$ of the Ca, there by advancing the structural stability of the system without clustering. Compared with the experimental $E_{coh}$ of the Ca bulk, the clustering of the Ca atom on the defective $C_3$NNT can be prevented. Based on the $E_{bind}$, the *Cv* structure is the best host material for the Ca atom. The large $E_{bind}$ values demonstrate that newly formed Ca–N and Ca–C bonds are quite strong.

As found from Table 1, the difference in the Fermi level of the defective and non-defective $C_3$NNT in the presence and absence of the Ca atom was interpreted by the CT between the metal atom and the nanotube within the adsorption process. The Φ value for the *perfect*, *Cv*, and *Nv* structures was obtained 2.28, 2.15, and 2.20 eV, respectively. Electron emission from the nanotubes surface in the presence of an electric field is increasing by decreasing the Φ value [35]. Therefore, the Ca atom can increase the field emission current of the $C_3$NNT by reducing the Φ value.

### *Hydrogen adsorption on the Ca-decorated $C_3$NNT*

To find high-capacity hydrogen storage materials, the Ca-decorated perfect and defective $C_3$NNTs were examined by sequentially adding individual $H_2$ molecules. The maximum number of adsorbed $H_2$ molecule per Ca atom in the *perfect*, *Cv*, and *Nv* structures are five (−0.08 eV/$H_2$), eight (−0.11 eV/$H_2$), and seven (−0.11 eV/$H_2$), respectively (see Fig. 2 and Table 2). As summarized in Table 2, average distance between Ca and H atoms and adsorption energy are increased and decreased, respectively, respect to those values in Table 3. Furthermore, the maximum $E_{ads}$ was achieved by four, four, and three $H_2$ molecules adsorbed on the *Ca@perfect*, *Ca@Cv*, and *Ca@Nv*, respectively (see Fig. 3), as tabulated in Table 3. The results indicated that the pristine form in the presence of the Ca atom has a small $E_{ads}$ (−0.09 eV/$H_2$) which is categorized as van der Waals (vdW) interaction. This energy is greater than the typical vdW interaction energy of ~0.05 eV, but still smaller

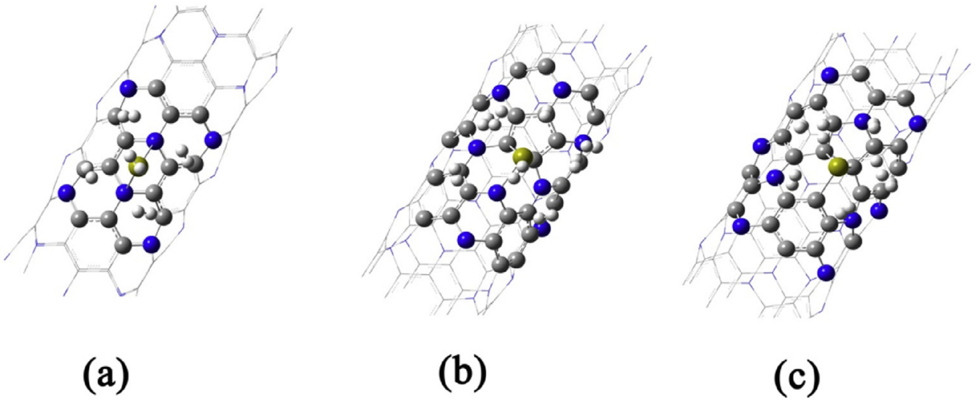

**Fig. 2 – The optimized structures of (a) Ca@perfect + $5H_2$, (b) Ca@Cv + $8H_2$, (c) Ca@Nv + $7H_2$. Gray, blue, white, and green colors are represented carbon, nitrogen, hydrogen, and calcium atoms, respectively. (For interpretation of the references to color in this figure legend, the reader is referred to the web version of this article.)**

**Table 2 – Structural parameters for the structures with the maximum number of hydrogen atoms. Average distance between Ca and H atoms $d_{av}$(Ca–H), average bond length in $H_2$ $L_{av}$(H–H), and adsorption energy ($E_{ads}$).**

| System | $d_{av}$(Ca–H) (Å) | $L_{av}$(H–H) (Å) | $E_{ads}$ (eV) |
|---|---|---|---|
| Ca@perfect + $5H_2$ | 2.73 | 0.76 | −0.08 |
| Ca@$C_v$ + $8H_2$ | 3.15 | 0.75 | −0.11 |
| Ca@$N_v$ + $7H_2$ | 3.06 | 0.75 | −0.11 |

than the requirement for the storage near room temperature around 0.20 eV [16]. As is well-known, the GGA reduces the absolute $E_{ads}$ about 25% [16,52]. By consideration of this deviation, the actual $E_{ads}$ is expected to be somewhat around −0.09, −0.18, and −0.17 eV/$H_2$ for the *Ca@perfect*, *Ca@Cv*, and *Ca@Nv*, respectively. Nguyen et al. showed that the average $E_{ads}$ of $H_2$ on the Ca-decorated CNT is in the range of 0.08–0.13 eV/$H_2$ [16]. Interestingly, the number of $H_2$ adsorbed on the Ca atom on the $C_V$ structure almost 1.6 times more than on the Ca atom on mono-vacancy CNT [10]. Compare with Ca-decorated graphene, CNT, $C_{60}$, $BC_7$, $BC_2N$, boron sheet, the $C_3$NNT seems to be a suitable candidate for hydrogen storage purpose [10,17,29,33,34,37].

Turning now to the bonding mechanism and CT between the complexes and $H_2$ molecules, as indicated in Table 3, a donation (i.e. hybridization between the occupied $H_2$ $\sigma$ orbital and the empty Ca *d* orbital) and back-donation (i.e. the hybridization between the occupied Ca *s* and *d* orbitals and the empty $H_2$ antibonding ($\sigma^*$) orbital) have been occurred in the perfect form. Since the Ca atom loses more electrons in the *Ca@Cv* (26% of valance electrons) and *Ca@Nv* structures (23% of valance electrons), the Ca atom just prefers to get electrons from the neighboring atoms. Therefore, donation and back-donation mechanism cannot be observed between $H_2$ molecules and the *Ca@Cv* and *Ca@Nv* complexes. Longer distance between $H_2$ molecules and the Ca atom in comparison with the titanium (Ti) as a TM can be interpreted by above descriptions. The nearest distances between Ca atom and a H atom in $H_2$ molecules vary between 2.41 and 2.74 Å whereas the minimum distance between Ti atom to H atom are from 1.72 to 1.95 Å [5,12]. The separation of H atoms in $H_2$ molecules is much smaller than that of the TM atom case (typically more than 25%) [5,12]. The average bond lengths of $H_2$ molecules on the *Ca-perfect*, *Ca@Cv*, and *Ca@Nv* are 0.77, 0.76, and 0.76 Å, respectively, which are slightly stretched from the isolated $H_2$ molecule (0.75 Å).

For deep understanding, PDOS can help us to analysis of orbital hybridization between adsorbent and adsorbate. As shown in Fig. 3 (left panel), the $H_2$ molecules are binded with the complexes via the hybridization of the *d* states of the Ca atom with the $H_2$ states. This hybridization was observed for all the three cases. As a result, these interactions can be explained by Kubas interaction. In Fig. 3(a) peaks in bottom and above Fermi level confirmed that a donation and back donation in the complex are occurred. The peaks center

**Table 3 – Structural and electronic parameters for the structures with the maximum adsorption energy. Calculated minimum distance of Ca atom to the nanotube $d_{min}$(Ca-nanotube), average distance between Ca and H $d_{av}$(Ca–H), average bond length in $H_2$ $L_{av}$(H–H), adsorption energy ($E_{ads}$), charge transfer of s, p, and d orbital of Ca atom ($CT_{(s)}$), ($CT_{(p)}$), and ($CT_{(d)}$), respectively, and net charge transfer for Ca atom (CT (Ca)). A negative value for CT indicates that the Ca atom lose charge density.**

| System | $d_{min}$(Ca-nanotube) (Å) | $d_{av}$(Ca–H) (Å) | $L_{av}$(H–H) (Å) | $E_{ads}$ (eV) | $CT_{(s)}$ \|e\| | $CT_{(p)}$ \|e\| | $CT_{(d)}$ \|e\| | CT (Ca) \|e\| |
|---|---|---|---|---|---|---|---|---|
| Ca@perfect + $4H_2$ | 2.40 | 2.45 | 0.77 | −0.09 | −0.57 | 0.00 | +0.53 | −0.04 |
| Ca@$C_v$ + $4H_2$ | 2.25 | 2.59 | 0.76 | −0.15 | +0.03 | 0.00 | +0.14 | +0.17 |
| Ca@$N_v$ + $3H_2$ | 2.28 | 2.64 | 0.76 | −0.13 | −0.01 | 0.00 | +0.11 | +0.10 |

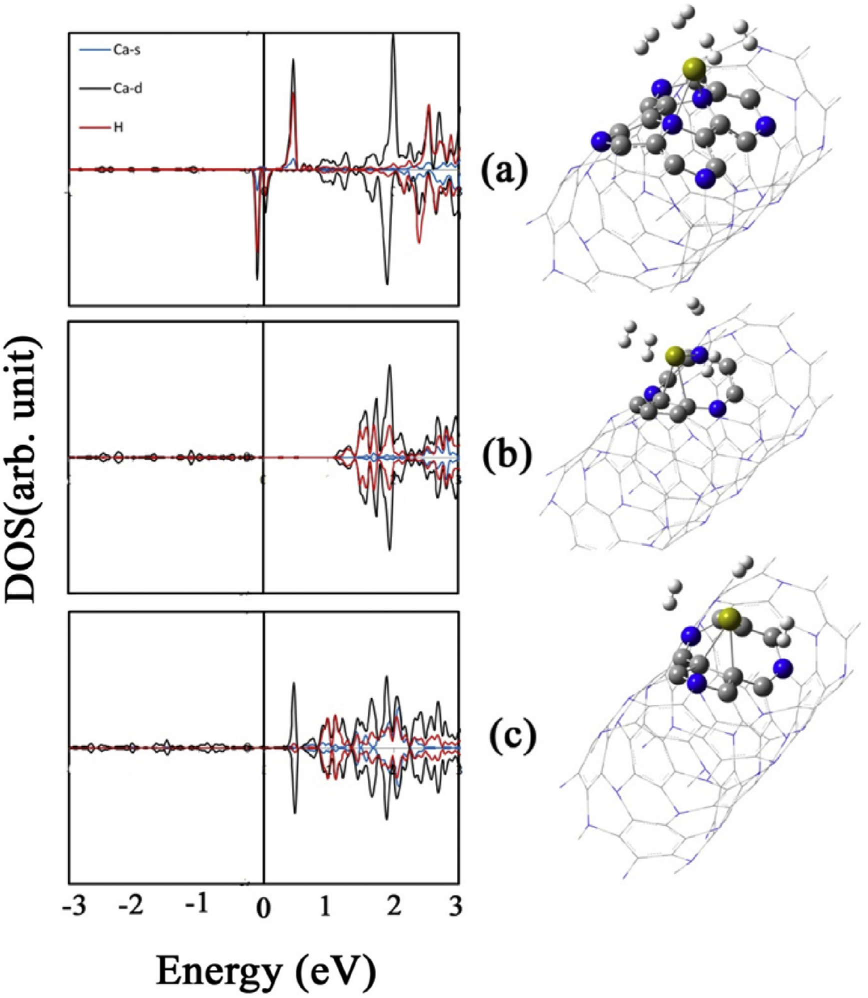

**Fig. 3 – Left panel: Partial density of states (PDOS) for (a) Ca@perfect + $4H_2$, (b) Ca@Cv + $4H_2$, (c) Ca@Nv + $3H_2$. Right panel: The optimized structures of corresponding structures are represented in front of each PDOSs. Gray, blue, white, and green colors are represented carbon, nitrogen, hydrogen, and calcium atoms, respectively. Fermi level is set to zero. (For interpretation of the references to color in this figure legend, the reader is referred to the web version of this article.)**

around −0.5 to 0 eV correspond to the hybridization of the Ca 3*d* with the $H_2$ $\sigma^*$ orbitals. As shown in Fig. 3 (b) and (c), there aren't any significant peaks bottom Fermi level. In other hand, strong hybridization is evident in range of 1–3 eV. Therefore, our analysis showed that the large $E_{ads}$ is related to the structures with the most hybridization between frontier orbital molecules.

## Conclusion

In brief, we demonstrated the possibility of adsorption of the Ca atom on the perfect and defective $C_3NNT$. The results showed that the new complexes can serve as a high-capacity hydrogen storage medium. The electronic and structural parameters were obtained. Interaction between Ca atom and the nanotubes and $H_2$ molecules are explained by Dewar coordination and Kubas interaction, respectively. It is noted that, the Ca atom has a much lower tendency for clustering on the defective nanotubes. In order to hydrogen storage, we encourage the experimental scientists to synthesize these nanomaterials that may operate at ambient condition.

## Acknowledgments

Computations were performed on the GPC supercomputer at the SciNet HPC Consortium. SciNet is funded by: the Canada Foundation for Innovation under the auspices of Compute Canada; the Government of Ontario; Ontario Research Fund – Research Excellence; and the University of Toronto. Further, we are grateful to Sanandaj Branch, Islamic Azad University Council for the financial support of this research.

## REFERENCES

[1] Züttel A, Sudan P, Mauron P, Kiyobayashi T, Emmenegger C, Schlapbach L. Hydrogen storage in carbon nanostructures. Int J Hydrogen Energy 2002;27:203–12.

[2] Panella B, Hirscher M, Roth S. Hydrogen adsorption in different carbon nanostructures. Carbon 2005;43:2209–14.
[3] Dillon A, Jones K, Bekkedahl T, Kiang C, Bethune D, Heben M. Storage of hydrogen in single-walled carbon nanotubes. Nature 1997;386:377–9.
[4] Sahaym U, Norton MG. Advances in the application of nanotechnology in enabling a ‘hydrogen economy’. J Mater Sci 2008;43:5395–429.
[5] Yildirim T, Ciraci S. Titanium-decorated carbon nanotubes as a potential high-capacity hydrogen storage medium. Phys Rev Lett 2005;94:175501.
[6] Gallouze M, Kellou A, Drir M. Electronic and magnetic properties of adsorbed $H_2$ on graphene with atomic defects: ab initio study. Phys E Low-dimensional Syst Nanostructures 2013;52:127–35.
[7] Fair K, Cui X, Li L, Shieh C, Zheng R, Liu Z, et al. Hydrogen adsorption capacity of adatoms on double carbon vacancies of graphene: a trend study from first principles. Phys Rev B 2013;87:014102.
[8] Kim G, Jhi S-H, Lim S, Park N. Effect of vacancy defects in graphene on metal anchoring and hydrogen adsorption. Appl Phys Lett 2009;94:173102.
[9] Ma L, Zhang J-M, Xu K-W, Ji V. Hydrogen adsorption and storage of Ca-decorated graphene with topological defects: a first-principles study. Phys E Low-dimensional Syst Nanostructures 2014;63:45–51.
[10] Lee H, Ihm J, Cohen ML, Louie SG. Calcium-decorated carbon nanotubes for high-capacity hydrogen storage: first-principles calculations. Phys Rev B 2009;80:115412.
[11] Lee H, Ihm J, Cohen ML, Louie SG. Calcium-decorated graphene-based nanostructures for hydrogen storage. Nano Lett 2010;10:793–8.
[12] Jalili S, Molani F, Schofield J. Ti-coated BC2N nanotubes as hydrogen storage materials. Can J Chem 2013;91:1–7.
[13] Lee S, Lee M, Choi H, Yoo DS, Chung Y-C. Effect of nitrogen induced defects in Li dispersed graphene on hydrogen storage. Int J Hydrogen Energy 2013;38:4611–7.
[14] Ao Z, Peeters F. Electric field activated hydrogen dissociative adsorption to nitrogen-doped graphene. J Phys Chem C 2010;114:14503–9.
[15] Ao Z, Hernandez-Nieves A, Peeters F, Li S. The electric field as a novel switch for uptake/release of hydrogen for storage in nitrogen doped graphene. Phys Chem Chem Phys 2012;14:1463–7.
[16] Nguyen MC, Cha MH, Bae J, Kim Y, Kim M, Ihm J. Calcium-decorated, hydroxylated single-walled carbon nanotubes for hydrogen storage: a first-principles study. ChemPhysChem 2011;12:777–80.
[17] Yoon M, Yang S, Hicke C, Wang E, Geohegan D, Zhang Z. Calcium as the superior coating metal in functionalization of carbon fullerenes for high-capacity hydrogen storage. Phys Rev Lett 2008;100:206806.
[18] Chen P, Wu X, Lin J, Tan K. High H2 uptake by alkali-doped carbon nanotubes under ambient pressure and moderate temperatures. Science 1999;285:91–3.
[19] Sun Q, Jena P, Wang Q, Marquez M. First-principles study of hydrogen storage on Li12C60. J Am Chem Soc 2006;128:9741–5.
[20] Sun Q, Wang Q, Jena P, Kawazoe Y. Clustering of Ti on a C60 surface and its effect on hydrogen storage. J Am Chem Soc 2005;127:14582–3.
[21] Zou X, Cha M-H, Kim S, Nguyen MC, Zhou G, Duan W, et al. Hydrogen storage in Ca-decorated, B-substituted metal organic framework. Int J Hydrogen Energy 2010;35:198–203.
[22] Gopalsamy K, Subramanian V. Hydrogen storage capacity of alkali and alkaline earth metal ions doped carbon based materials: a DFT study. Int J Hydrogen Energy 2014;39:2549–59.
[23] López-Corral I, de Celis J, Juan A, Irigoyen B. DFT study of H2 adsorption on Pd-decorated single walled carbon nanotubes with C-vacancies. Int J Hydrogen Energy 2012;37:10156–64.
[24] Park H-L, Yi S-C, Chung Y-C. Hydrogen adsorption on Li metal in boron-substituted graphene: an ab initio approach. Int J Hydrogen Energy 2010;35:3583–7.
[25] Mananghaya M. Hydrogen adsorption of novel N-doped carbon nanotubes functionalized with Scandium. Int J Hydrogen Energy 2015;40:9352–8.
[26] Naghshineh N, Hashemianzadeh M. First-principles study of hydrogen storage on Si atoms decorated C 60. Int J Hydrogen Energy 2009;34:2319–24.
[27] Rao D, Wang Y, Meng Z, Yao S, Chen X, Shen X, et al. Theoretical study of H2 adsorption on metal-doped graphene sheets with nitrogen-substituted defects. Int J Hydrogen Energy 2015;40:14154–62.
[28] Yang X, Zhang R, Ni J. Stable calcium adsorbates on carbon nanostructures: applications for high-capacity hydrogen storage. Phys Rev B 2009;79:075431.
[29] Lei X, Liu G, Wu M, Xu B, Ouyang C, Pan B. Hydrogen storage on calcium-decorated BC7 sheet: a first-principles study. Int J Hydrogen Energy 2014;39:2142–8.
[30] Sorokin PB, Lee H, Antipina LY, Singh AK, Yakobson BI. Calcium-decorated carbyne networks as hydrogen storage media. Nano Lett 2011;11:2660–5.
[31] Wang YS, Yuan PF, Li M, Jiang WF, Sun Q, Jia Y. Calcium-decorated graphyne nanotubes as promising hydrogen storage media: a first-principles study. J Solid State Chem 2013;197:323–8.
[32] Olguin M, Baruah T, Zope RR. Calcium coated B80 fullerene: a study on various coating configurations of B80. Chem Phys Lett 2011;514:66–9.
[33] Beheshti E, Nojeh A, Servati P. A first-principles study of calcium-decorated, boron-doped graphene for high capacity hydrogen storage. Carbon 2011;49:1561–7.
[34] Wang J, Du Y, Sun L. Ca-decorated novel boron sheet: a potential hydrogen storage medium. Int J Hydrogen Energy 2016;41:5276–83.
[35] Kittel C. Introduction to solid state physics. 8th ed. John Wiley & Sons; 2005.
[36] Chan KT, Neaton J, Cohen ML. First-principles study of metal adatom adsorption on graphene. Phys Rev B 2008;77:235430.
[37] Qiu N-x, Tian Z-y, Guo Y, Zhang C-h, Luo Y-p, Xue Y. A first-principle study of calcium-decorated BC2N sheet doped by boron or carbon for high hydrogen storage. Int J Hydrogen Energy 2014;39:9307–20.
[38] Lee S, Lee M, Chung Y-C. Enhanced hydrogen storage properties under external electric fields of N-doped graphene with Li decoration. Phys Chem Chem Phys 2013;15:3243–8.
[39] Czerw R, Terrones M, Charlier JC, Blase X, Foley B, Kamalakaran R, et al. Identification of electron donor states in N-doped carbon nanotubes. Nano Lett 2001;1:457–60.
[40] Hales J, Barnard AS. Thermodynamic stability and electronic structure of small carbon nitride nanotubes. J Phys Condens Matter 2009;21:144203.
[41] Jalili S, Molani F, Akhavan M, Schofield J. Role of defects on structural and electronic properties of zigzag $C_3N$ nanotubes: a first-principle study. Phys E Low-dimensional Syst Nanostructures 2014;56:48–54.
[42] Molani F, Jalili S, Schofield J. Computational study of interaction of alkali metals with C3N nanotubes. J Mol Model 2015;21:1–7.
[43] Bagheri Z. DFT study on the chemical sensitivity of C3N nanotubes toward acetone. Phys E Low-dimensional Syst Nanostructures 2016;76:151–7.

[44] Giannozzi P, Baroni S, Bonini N, Calandra M, Car R, Cavazzoni C, et al. QUANTUM ESPRESSO: a modular and open-source software project for quantum simulations of materials. J Phys Condens Matter 2009;21:395502.

[45] Perdew JP, Burke K, Ernzerhof M. Generalized gradient approximation made simple. Phys Rev Lett 1996;77:3865–8.

[46] Monkhorst HJ, Pack JD. Special points for Brillouin-zone integrations. Phys Rev B 1976;13:5188–92.

[47] Löwdin PO. On the non-orthogonality problem connected with the use of atomic wave functions in the theory of molecules and crystals. J Chem Phys 1950;18:365–75.

[48] Mingos DMP. A historical perspective on Dewar's landmark contribution to organometallic chemistry. J Organomet Chem 2001;635:1–8.

[49] Zhu J, Farmer JA, Ruzycki N, Xu L, Campbell CT, Henkelman G. Calcium adsorption on MgO (100): energetics, structure, and role of defects. J Am Chem Soc 2008;130:2314–22.

[50] Gao B, Zhao J-x, Cai Q-h, Wang X-g, Wang X-z. Doping of calcium in C60 fullerene for enhancing CO2 capture and N2O transformation: a theoretical study. J Phys Chem A 2011;115:9969–76.

[51] Hwang HJ, Kwon Y, Lee H. Thermodynamically stable calcium-decorated graphyne as a hydrogen storage medium. J Phys Chem C 2012;116:20220–4.

[52] Lee H, Choi WI, Ihm J. Combinatorial search for optimal hydrogen-storage nanomaterials based on polymers. Phys Rev Lett 2006;97:056104.